

Optical potential parameters from $^{12}\text{C} + \text{Zr}$ elastic scattering

L. Gan^{1,2,a}, Z. H. Li^{1,b}, H. B. Sun², J. Su¹, Y. J. Li¹, S. Q. Yan¹, Y. B. Wang¹, S. Zeng¹, X. X. Bai¹, X. C. Du¹, Z. D. Wu¹, S. J. Jin¹, W. J. Zhang¹, W. P. Liu¹, and E. T. Li²

¹China Institute of Atomic Energy, P.O. Box 275(10), Beijing 102413, China

²Shenzhen University, Shenzhen 518060, China

Abstract. The angular distributions of $^{12}\text{C} + ^{90,92,94,96}\text{Zr}$ elastic scattering were measured with the Q3D magnetic spectrometer at the HI-13 tandem accelerator, Beijing. The real part of optical potential were extracted by analysing these angular distributions. The analysis enable us to avoid the influence of Coulomb effect and to observe the dependence of optical potential on the nuclear properties. With the deduced potential parameters, the experimental elastic scattering angular distributions can be reproduced very well. Formulas to infer global heavy-ion potential parameters were obtained then by analyzing the extracted optical potential parameters. The formulas can be used widely in heavy-ion nuclear reactions.

1 Introduction

The nucleus-nucleus potential is a key component in any analysis of nuclear reactions, and can be used to estimate the cross sections of different nuclear reactions[1–4]. It has been of great interest to study the optical potential in heavy ion physics for many years[1–10]. The potential consists of nuclear, Coulomb, and centrifugal components. The Coulomb and centrifugal interactions of two nuclei are well known, but the nuclear component is far from being fully understood[11, 12]. The nuclear component of the interaction potential is often parameterized by the optical potential, and have the Woods-Saxon shape[13–15]. The real part of the optical potential can be extracted by fitting the elastic scattering angular distributions[16]. However, the optical potential parameters always have large ambiguities[12, 17].

Since the strong Coulomb interaction between heavy-ions will interfere us to extract the exact potential information, it is important to overcome the effects of interference in the optical potential analysis. In the present work, angular distributions of the elastic scattering for ^{12}C from four zirconium isotopes ($^{90,92,94,96}\text{Zr}$) were measured. The collision systems have the same Coulomb interaction, we can therefore extracted the potential parameters corresponding to the nuclear interaction information from the angular distributions.

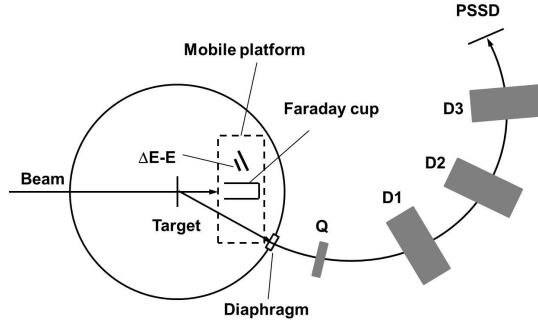


Figure 1. Experimental settings

2 Experiment

The measurements were performed with the Q3D magnetic spectrometer at the HI-13 tandem accelerator in China Institute of Atomic Energy(CIAE), Beijing. The experimental settings is shown in Fig.1. The ^{12}C beam with the energy of 66.0 MeV from the accelerator impinged on the carbon-supported zirconium enriched isotopes targets of ZrO_2 . The thicknesses of the targets are about $35 \mu\text{g}/\text{cm}^2$. A movable Faraday cup was placed behind the target to monitor the beam intensity, and to count the incident ions. On the left side of Faraday cup, a ΔE -E detector telescopic system was set for the aim of beam's relatively normalizing. The accepted solid angle of Q3D magnetic spectrometer was set to be 0.34 msr for good angular resolution. The reaction products were focused and separated by Q3D and then measured by a $50 \text{ mm} \times 50 \text{ mm}$ two-dimensional position-sensitive silicon detector (PSSD) at the focal plane. The two-dimensional position information from the PSSD enabled the products emitted into the accepted solid angle of Q3D to be fully recorded, and the corresponding energy signals were used to remove the impurities with the same magnetic rigidity. The high momentum resolution of Q3D enable us to identify the events from different isotopes in the targets at the angular region of $\theta_{\text{lab}} > 20^\circ$.

The typical two-dimensional spectrum of kinetic energy versus the horizon position for $^{12}\text{C} + ^{94}\text{Zr}$ elastic scattering at 14° is shown in Fig.2. One can see that, the object ions from the reactions can be clearly identified via the energy and position information. The position spectrum of object ions is also exhibited in the right part of Fig.2. The uncertainties of differential cross sections are mainly from the statistics and nonuniformity of the target thickness.

3 Extraction of the optical potential parameters

The central potential acting between the centers of mass of the nuclei is usually assumed to be the sum of Coulomb, nuclear, and centrifugal terms, which is expressed by

$$V(r) = V_c(r) + V_n(r) + V_l(r). \quad (1)$$

^ae-mail: ganlin2007@hotmail.com

^be-mail: zhli@ciae.ac.cn

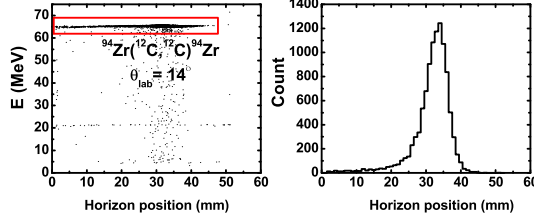


Figure 2. (colour online) The two-dimensional spectrum of kinetic energy versus the horizon position (left) and the horizon position spectrum of object ions (right) for $^{12}\text{C} + ^{94}\text{Zr}$ elastic scattering at 14°

The Coulomb potential corresponding to a uniform distribution of charge for $r < R_c$ and zero for $r > R_c$ is

$$V_c(r) = \begin{cases} \frac{Z_1 Z_2 e^2}{2R_c} \left(3 - \frac{r^2}{R_c^2}\right) & r < R_c \\ \frac{Z_1 Z_2 e^2}{r} & r > R_c \end{cases} \quad (2)$$

The nuclear potential is often described by the Woods-Saxon (WS) form:

$$V_n(r) = \frac{V}{1 + e^{(r-R_v)/a_v}} + \frac{iW}{1 + e^{(r-R_w)/a_w}} \quad (3)$$

which is defined by six parameters: the depth, the radius and the diffuseness for both real and imaginary components.

The centrifugal potential is related to the angular momentum l by

$$V_l(r) = \frac{l(l+1)\hbar^2}{2\mu r^2}. \quad (4)$$

In the above expressions, R_c , R_v and R_w are the interaction radius for the corresponding potential, and can be calculated by the radius parameters: $R_i = r_i(A_1^{1/3} + A_2^{1/3})$, $i = C, V, W$. $Z_{1,2}$ and $A_{1,2}$ are the numbers of protons and nucleons in the corresponding nuclei, e in eq.(2) is the proton charge. a_v and a_w are the nuclear diffuses, μ is the reduced mass of the system.

The calculated cross section near the Coulomb barrier was found not to be sensitive to the parameter R_c , thus r_c was set equal to 1.0 throughout these calculations. The parameters of the imaginary potential, W , r_w and a_w are relatively insensitive to the angular distributions of elastic scattering, the values of $W = 35$ MeV, $r_w = 1.22$ fm and $a_w = 0.47$ fm were used in the follow calculations.

Firstly, the three parameters of V , r_v and a_v were varied in the regions of 10-280 MeV, 1.0-1.5 fm and 0.35-0.8 fm, by steps of 1 MeV, 0.01 fm and 0.01 fm respectively. The four angular distributions of the elastic scattering were calculated with all these parameter combinations, and the corresponding χ^2 were obtained too.

Secondly, the most suitable a_v for the four elastic scattering reactions can be found from figures of χ^2 versus a_v . Such as Fig.3, $a_v = 0.55$ fm is extracted for $^{12}\text{C} + ^{92}\text{Zr}$ elastic scattering.

Thirdly, for the interaction between heavy ions, according to the "Igo ambiguity"[18], the angular distributions calculated with different parameter sets can reproduce the experimental angular distribution of the elastic scattering. As shown in Fig.4, the parameter sets at the bottom of each curve can fit $^{12}\text{C} + ^{94}\text{Zr}$ elastic scattering well. The relationship between V , r_v and a_v of these parameter sets is as follow:

$$V \times \exp(R_v/a_v) = \text{const} \quad (5)$$

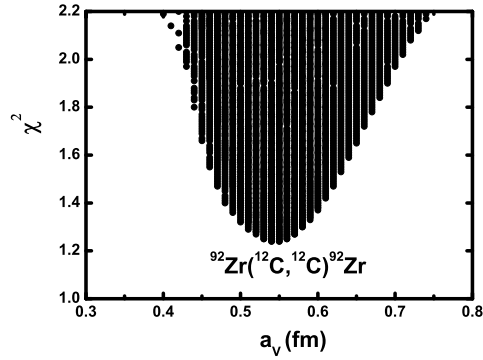


Figure 3. χ^2 versus a_v for $^{12}\text{C} + ^{92}\text{Zr}$ elastic scattering.

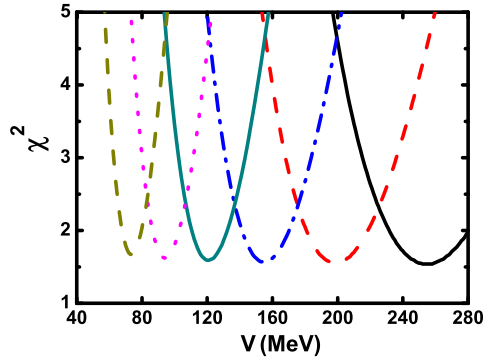


Figure 4. (Color online) χ^2 versus V for $^{12}\text{C} + ^{94}\text{Zr}$ elastic scattering. Each curve responding a value of r_v . From left to right, the values of r_v are from 1.20 to 1.10 fm respectively, step is 0.02 fm.

With the value of const in eq.(5) gained, and a_v fixed, the relationship between V and r_v was obtained.

Fourthly, volume integration analysis was introduced to find r_v . The form of volume integration is given in the following equation[19].

$$\begin{aligned} J_V &= 348.44 \times \exp(-0.00739 \times E/A_1) \\ &= \frac{4\pi}{A_1 A_2} \int \frac{r^2 V}{1 + \exp((r - R_V)/a_v)} dr \end{aligned} \quad (6)$$

According to eq.(7), with a_v fixed, another relationship between V and r_v was found.

With these two relationship between V and r_v , one can see from Fig.5, V and r_v are found at the point of intersection.

The values of V , r_v and a_v for $^{12}\text{C} + ^{90,92,94,96}\text{Zr}$ elastic scatterings are listed in Table 1.

The angular distributions of $^{12}\text{C} + ^{90,92,94,96}\text{Zr}$ elastic scattering calculated with these parameters listed in Table 1 are shown in Fig.6.

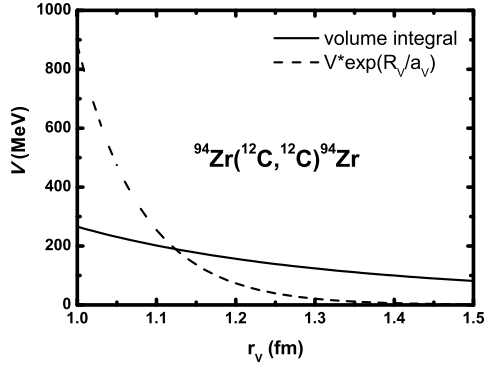


Figure 5. V versus r_v in eq.(5) (line) and eq.(7) (dot) for $^{12}\text{C} + ^{94}\text{Zr}$ elastic scattering.

Table 1. V , r_v and a_v for $^{12}\text{C} + ^{90,92,94,96}\text{Zr}$ elastic scattering

	^{90}Zr	^{92}Zr	^{94}Zr	^{96}Zr
V (MeV)	194.4	192	189	186
r_v (fm)	1.108	1.116	1.124	1.133
a_v (fm)	0.55	0.55	0.55	0.55
$V * e^{(R_v/a_v)}$ (MeV)	1.63×10^8	1.89×10^8	2.21×10^8	2.59×10^8

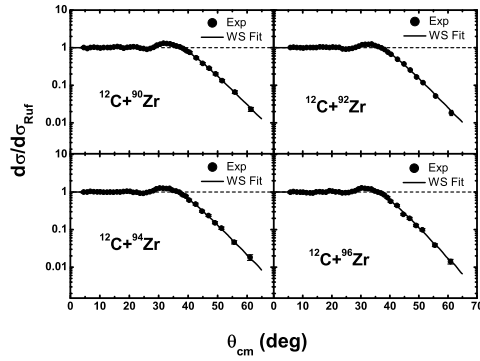


Figure 6. The experimental angular distributions of $^{12}\text{C} + ^{90,92,94,96}\text{Zr}$ elastic scattering (dots) and the corresponding Woods-Saxon fits (lines). It is obvious that, the calculated angular distributions can fit the experimental data well.

It is easy to be found that the values of V and r_v versus R_v both represent good linearity, as shown in Fig.7.

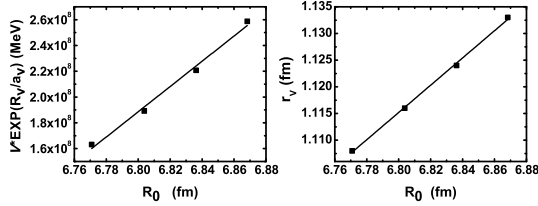


Figure 7. V versus R_v (left) and r_v versus R_v (right) for $^{12}\text{C} + ^{90,92,94,96}\text{Zr}$ elastic scattering reactions. Linear fits were performed too.

The global heavy-ion optical potential parameters is given by following formulas:

$$\begin{aligned}
 V &= -86.8(A_1^{1/3} + A_2^{1/3}) + 779.7 \text{ MeV} \\
 r_v &= 0.2555(A_1^{1/3} + A_2^{1/3}) - 0.617 \text{ fm} \\
 a_v &= 0.55 \text{ fm}
 \end{aligned}
 \tag{7}$$

Use the potential parameters obtained from the above formulas, we can calculate the experimental data of $^{16}\text{O} + ^{92}\text{Mo}$ [20], the incident energy of ^{16}O . One can see from Fig.8, the experimental angular distributions can be reproduced very well.

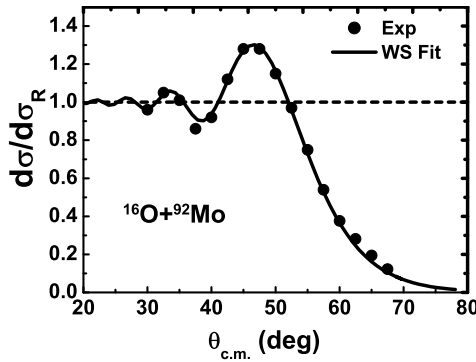


Figure 8. The angular distributions of $^{16}\text{O} + ^{92}\text{Mo}$ from references(dots) and calculated with WS potential parameters(line).

4 Conclusion

The angular distributions of $^{12}\text{C} + ^{90,92,94,96}\text{Zr}$ elastic scattering were measured with the Q3D magnetic spectrometer at the HI-13 tandem accelerator in CIAE. Hundreds of thousands optical potential parameter combinations were taken into the calculation of each elastic scattering reactions, and the

most suitable a_v was found to be 0.55 fm for $^{12}\text{C} + ^{90,92,94,96}\text{Zr}$ elastic scattering reactions from the figure of χ^2 versus a_v . V and r_v were then extracted with a_v fixed. The formulas to infer global heavy-ion potential parameters were obtained, and they are very useful not only for $^{12}\text{C}+\text{Zr}$, but also for others.

We acknowledge the staff of HI-13 tandem accelerator for the smooth operation of the machine, and N. K. Timofeyuk and R. C. Johnson for their helpful discussions on DWBA calculations and charge symmetry. We are grateful to the anonymous referee for helpful comments. This work was performed with the support of the National Natural Science Foundation of China under Grant Nos. 11321064, 11075219, 11375269, 11275272 and 11275018, the 973 program of China under Grant No. 2013CB834406.

References

- [1] W. D. Myers and W. J. Świątecki, Phys. Rev. C **62**, 044610 (2000)
- [2] V. Y. Denisov, Phys. Lett. B **526**, 315 (2002)
- [3] W. M. Seif, J. Phys. G: Nucl. Part. Phys **30**, 1231 (2004)
- [4] V. Y. Denisov, Phys. Rev. C **89**, 044604 (2014)
- [5] B. Sinha, Phys. Rev. C **11**, 1546 (1975)
- [6] J. Fleckner and U. Mosel, Nulc. Phys. A **277**, 170 (1977)
- [7] T. Izumoto et al, Nulc. Phys. A **341**, 319 (1980)
- [8] N. Ohtsuka et al, Nulc. Phys. A **465**, 550 (1987)
- [9] D. T. Khoa, Nulc. Phys. A **484**, 376 (1988)
- [10] V. B. Soubbotin et al, Phys. Rev. C **64**, 014601 (2001)
- [11] M. Beckerman, Rep. Prog. Phys **51**, 1047 (1988)
- [12] A.T. Rudchik et al, Nulc. Phys. A **662**, 44 (2000)
- [13] D. A. Goldberg and S. M. Smith, Phys. Rev. Lett **29**, 8 (1972)
- [14] L. C. Chamon et al, Phys. Rev. C **66**, 014610 (2002)
- [15] K. S. Wilczyńska and J. Wilczyński, Phys. Rev. C **69**, 024611 (2004)
- [16] D. A. Goldberg and S. M. Smith, Phys. Rev. Lett **33**,12 (1974)
- [17] H. H. Gutbrod et al, Nulc. Phys. A **213**, 285 (1973)
- [18] G. Igo, Phys. Rev. **115**, 1665 (1959)
- [19] T. Furumoto et al., Phys. Rev. C **85**, 044607 (2012)
- [20] K. E. Rehm et al., Phys. Rev. C **12**, 1945 (1975)